Engineering Notes

Nonlinear Pressure Vessel Theory

EDWARD N. NELSON*
Arde Inc., Paramus, N. J.

Nomenclature

C_1, C_2 = constants
D = flexural rigidity, $Et^2/(1 - \nu^2)12$
E = modulus of elasticity
M = moment per unit length of circumference
P = radial load per unit length of circumference
p = pressure
R = radius
t = thickness
W = $[3(1 - \nu^2)]^{1/2}pR^2/2Et^2$
β = shell characteristic, $[3(1 - \nu^2)]^{1/4}/[Rt]^{1/2}$
δ = radial deflection
θ = rotational deflection
ν = Poisson's ratio
σ_H = hoop stress
σ_M = meridional stress

THIS note will tell what "the nonlinear pressure vessel theory" is, cite references[1-4] that present its mathematical development, and then show the results of using it on a number of practical problems. Additional references[5-8] for background information are included at the end of the note.

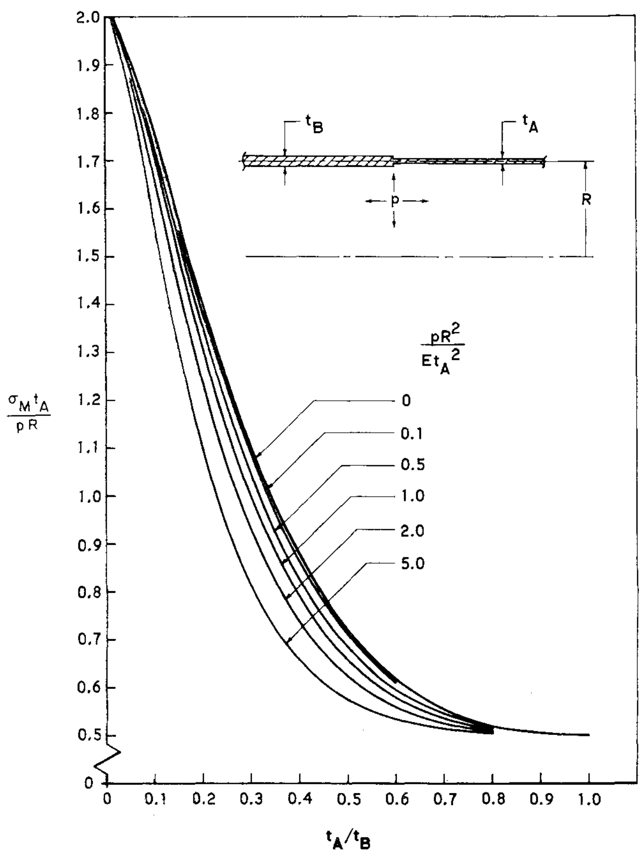

Fig. 1 Cylinder-to-cylinder juncture.

The deflection equations for a semi-infinite pressurized long cylinder at its edge are

$$\theta = -C_1M/D\beta + C_2P/2D\beta^2$$
$$\delta = C_2M/2D\beta^2 - C_1P/2D\beta^3 + (1 - \nu/2)pR^2/Et$$

where

$$C_1 = (1 - W)^{1/2}/(1 - 2W)$$
$$C_2 = 1/(1 - 2W)$$
$$W = [3(1 - \nu^2)]^{1/2}pR^2/2Et^2$$

when the effect of the meridional load $pR/2$ is also considered along with the edge moment M and the radial load P in the basic solution of this problem.[1] When the term pR^2/Et^2 is zero, then $C_1 = C_2 = 1$, and the more familiar linear pressure vessel equations are evolved. In all the figures subsequently presented in this note, a value of $\nu = 0.3$ is used.

When the juncture of two pressurized cylinders of different wall thicknesses, but with a common median line,[2] is investigated, and the attenuated stresses[3] are considered, then the maximum meridional and hoop stresses are found to occur in the thinner walled cylinder at some distance from the juncture. Figure 1 shows the maximum meridional stresses for this juncture problem for various values of the parameter pR^2/Et_A^2 and the thickness ratio, t_A/t_B. For this type of juncture, the maximum stresses decrease as the nonlinear parameter pR^2/Et_A^2 increases.

The problem of a 2:1 elliptical head-to-cylinder juncture has been investigated[4] using the linear theory. The stress patterns for this problem, when the nonlinear theory is used, are shown in Fig. 2. It was assumed that the nonlinear

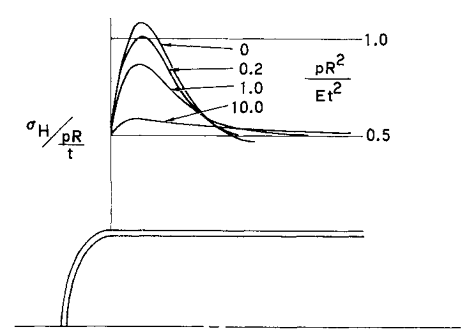

a) Hoop stress.

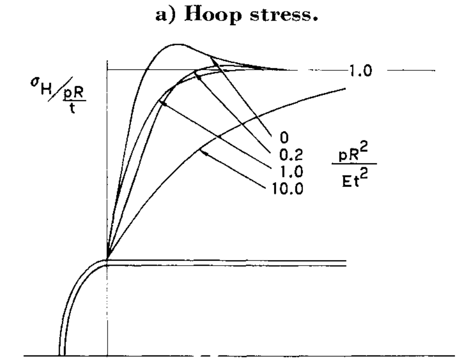

b) Meridinal stress.

Fig. 2 2:1 elliptical head-to-cylinder juncture.

Presented as Preprint 64-438 at the 1st AIAA Annual Meeting, Washington, D. C., June 29–July 2, 1964; revision received February 3, 1965.

* Senior Engineer. Member AIAA.

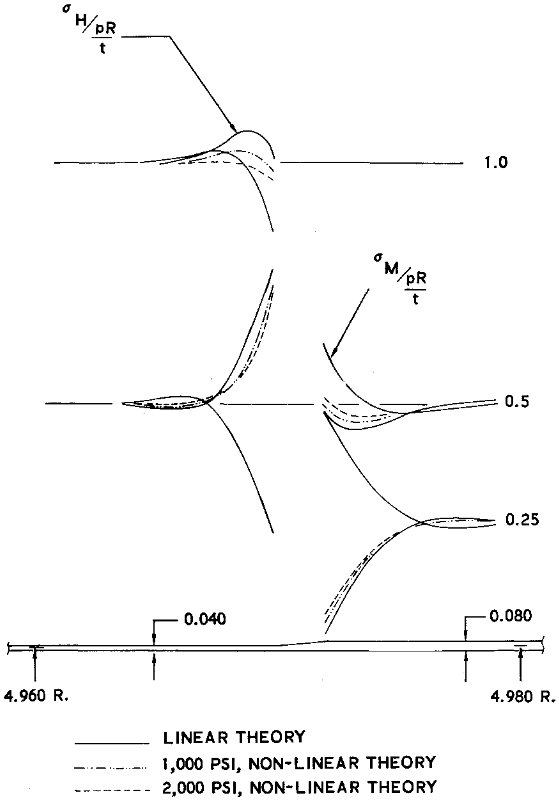

Fig. 3 Cylinder transition juncture.

equations that are valid for cylinders are a good first approximation for an ellipse. Figure 2 also shows that, as the parameter pR^2/Et^2 increases, the maximum stresses decrease.

Figures 3–5 show the effect of using the nonlinear theory on three practical juncture problems. The four stress patterns are shown for the linear theory; only the two outer radius stress patterns are shown for the nonlinear theory. In all three of these problems, the tapered transitions were approximated by a series of short cylinders whose equations are available.[1]

In Fig. 3, the maximum value of pR^2/Et^2 is 1.03, and the decrease in maximum hoop stress is most noticeable. In Figs. 4 and 5, the maximum value of pR^2/Et^2 is only 0.26, so that the decrease in maximum stresses is not as

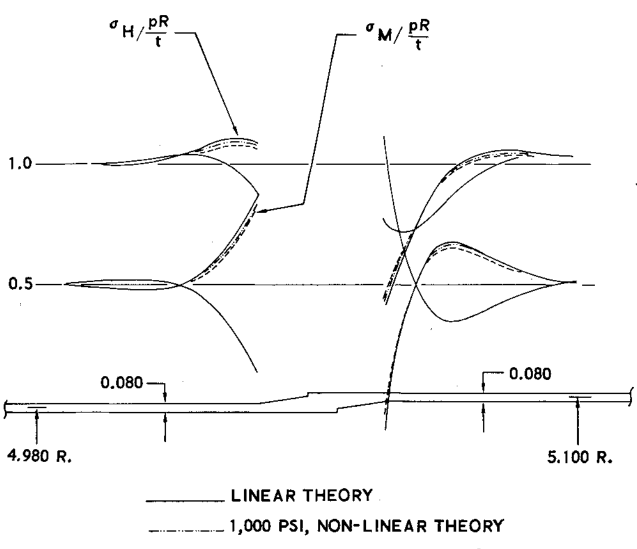

Fig. 4 Offset cylinder juncture.

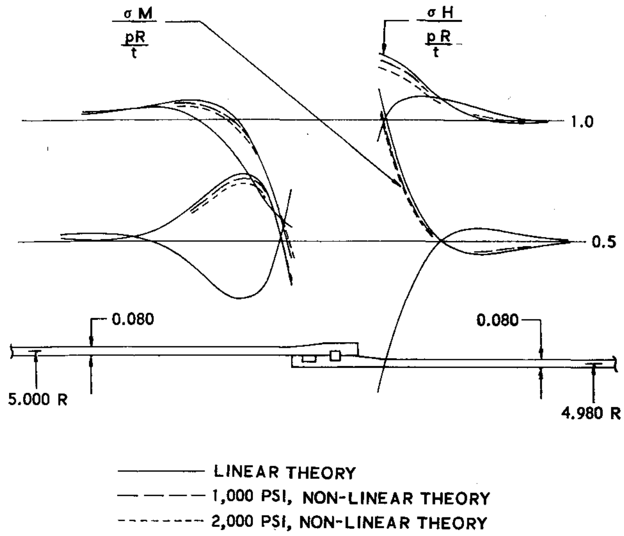

Fig. 5 Shear ring juncture.

large. Figures 3–5 illustrate the reduction in stress in three common missile case juncture problems. The reduction would be more noticeable if a 50-in.-diam case had been chosen rather than the 10-in.-diam case.

If the nonlinear theory is used to help design missile cases, the designer will probably encounter problems that involve geometric shapes that can only be approximated in the analysis; experimental testing may be required. Figures 3–5 show that the nonlinear effect may be too small to be checked satisfactorily by standard hydrostatic testing.

An interesting alternative method of pressure testing is available. So far only internal pressures have been considered, but the equations are also valid for external pressure, provided

$$p_{EXT} > Et^2/R^2(3[1 - \nu^2])^{1/2}$$

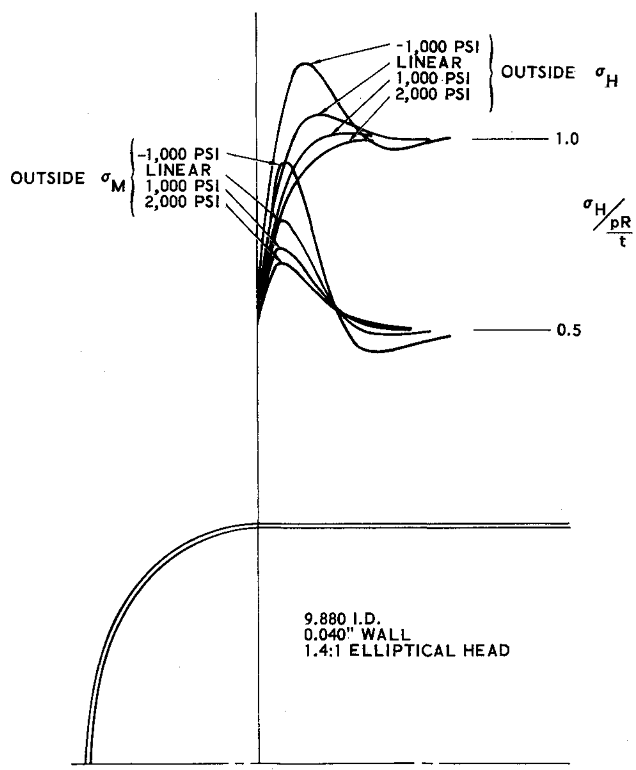

Fig. 6 1.4:1 elliptical head-to-cylinder juncture.

which is the buckling equation for a long cylinder. Figure 6 shows the nonlinear stress patterns for one external pressure and two internal pressure conditions for a 1.4:1 elliptical head-to-cylinder juncture. External pressure causes a more significant change in the maximum stress than will a corresponding internal pressure. Thus to check experimentally a particular theoretical juncture region, externally pressurizing the actual configuration or a smaller model may prove more feasible than the actual internal pressurization method.

The nonlinear pressure vessel theory enables a structure analyst to design lighter missile cases. In low-pressure space stations of the future the parameter pR^2/Et^2 may become high enough so that the nonlinear theory must be used.

References

[1] Hetenyi, M., *Beams on Elastic Foundation* (The University of Michigan Press, Ann Arbor, Mich., 1946), Chap. VI, pp. 127–135.

[2] Wilson, P. E. and Spier, E. E., "Nonlinear pressure coupling in cylindrical shell analysis," AIAA J. 2, 370–372 (1964).

[3] Grossman, W. B., "Investigation of maximum stresses in long, pressurized, cylindrical, shells," AIAA J. 1, 1129–1132 (1963).

[4] Timoshenko, S., *Theory of Plates and Shells* (McGraw-Hill Book Co., Inc., New York, 1940), 1st ed.

[5] Pulos, J. G. and Salerno, V. L., "Axisymmetric elastic deformations and stresses in a ring-stiffened, perfectly circular cylindrical shell under external hydrostatic pressure," David Taylor Model Basin Rept. 1497 (September 1961).

[6] Short, R. D. and Bart, R., "Analysis for determining stresses in stiffened cylindrical shells near structural discontinuities," David Taylor Model Basin Rept. 1065 (June 1959).

[7] Kempner, J. and Salerno, V. L., "Analysis of the inelastic behavior of transversely reinforced cylindrical shells under hydrostatic pressure," Polytechnic Institute of Brooklyn Aerodynamics Lab. PIBAL Rept. 172 (August 1950).

[8] Pulos, J. G., "Structural analysis and design considerations for cylindrical pressure hulls," David Taylor Model Basin Rept. 1639 (April 1963).

LITVC System Response Evaluation by Pressure Integration Methods

A. W. Langill Jr.
Aerojet-General Corporation, Sacramento, Calif.

THE injection of fluids into the diverging portion of rocket nozzles to obtain side force for vehicle guidance has received considerable attention over the past few years. To characterize the complete liquid injection thrust vector control (LITVC) system response under conditions of dynamic excitation, an injection program consisting of a series of variable frequency flow-rate oscillations, superimposed upon a steady-state level (Fig. 1), is often implemented. The problem is to measure, with reasonable accuracy, the sinusoidal flow-rate excitation and resulting side-force response.

The typical thrust stand used to constrain the solid rocket motor during captive testing is a lightly damped, multiple-degree-of-freedom spring-mass system exhibiting relatively low natural frequency parameters. Because of the poor damping qualities, the undistorted direct side-force measurement system bandwidth is limited to 10 or 25% of the lowest resonant frequency (depending upon the particular definition

Presented as Preprint 64-505 at the AIAA 1st Annual Meeting, Washington, D. C., June 29–July 2, 1964; revision received November 10, 1964.

* Technical Specialist, Solid Rocket Operations Test Division. Member AIAA.

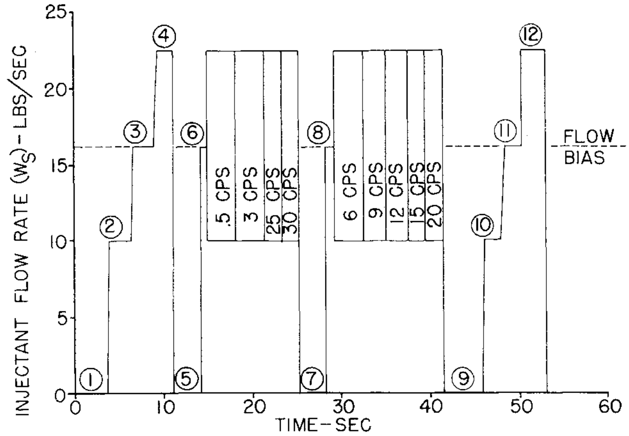

Fig. 1 Liquid injection program for dynamic response motor firing.

of "undistorted"). Since the maximum side-plane excitation frequency is often three or four times the lowest stand resonance, severe distortion in both amplitude and phase parameters occurs throughout the frequency range of interest. However, an indirect, instantaneous side-force measurement capability can be established by equating the side force to a corresponding internal nozzle-pressure integral. Total side force, due to liquid injection, is thus the sum of the pressure integral derived force level plus the momentum forces generated by the liquid.

Physical Test Environment

In the LITVC flow-rate program (Fig. 1), the initial and final portions consisted of a series of steady-state flow-rate null and plateau regions, whereas the intermediate portion was comprised of excitation frequencies extending from 0.5 to 30 cps. The time intervals allocated to data points 1–13 allowed an accurate direct side-force measurement; these program nulls provided a method for "calibrating" the corresponding pressure contour integral.

A multicomponent thrust stand was employed to constrain the solid rocket motor. In addition to the axial force cell, fore and aft side-plane force transducers were provided to measure the motor-generated side force. The use of modular flexure isolation and optimally sized force transducers resulted in relatively low thrust stand undamped natural frequency and damping characteristics.

A 52-nozzle-pressure-tap configuration (Fig. 2) provided the means for determining the internal nozzle-pressure distribution throughout the firing duration. All pressure taps were located in a single nozzle quadrant, thus insuring substantial coverage of a relative large geometric area. The

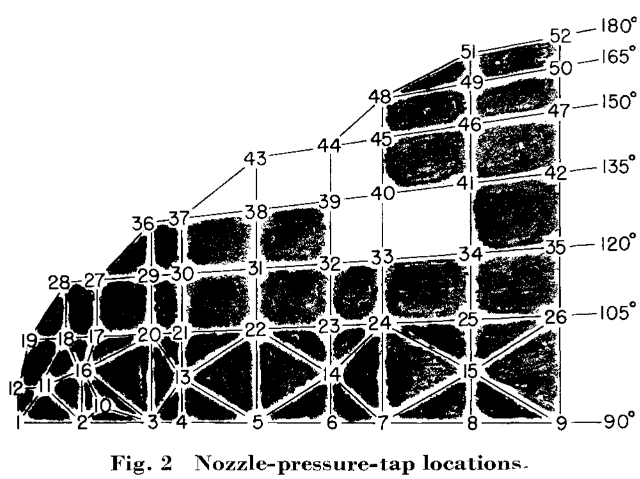

Fig. 2 Nozzle-pressure-tap locations.